A drug-resistant mutation in plant target of rapamycin validates the specificity of ATP -competitive TOR inhibitors in vivo

Romain Perdoux, Adam Barrada, Manal Boulaiz, Camille Garau, Clément Belbachir, Cécile Lecampion, Marie-hélène Montané, Benoît Menand

the plant journal

SEB SOCIETY FOR EXPERIMENTAL BIOLOGY

The Plant Journal (2023) doi: 10.1111/tpj.16564

A drug-resistant mutation in plant target of rapamycin validates the specificity of ATP-competitive TOR inhibitors *in vivo*

Romain Perdoux, Adam Barrada, Manal Boulaiz, Camille Garau, Clément Belbachir, Cécile Lecampion, Marie-Hélène Montané* and Benoît Menand*

Aix-Marseille Univ, CEA, CNRS, BIAM, LGBP Team, Marseille, France

Received 11 July 2023; revised 27 October 2023; accepted 13 November 2023.
*For correspondence (e-mail marie-helene.montane@univ-amu.fr; benoit.menand@univ-amu.fr).

SUMMARY

Kinases are major components of cellular signaling pathways, regulating key cellular activities through phosphorylation. Kinase inhibitors are efficient tools for studying kinase targets and functions, however assessing their kinase specificity *in vivo* is essential. The identification of resistant kinase mutants has been proposed to be the most convincing approach to achieve this goal. Here, we address this issue in plants via a pharmacogenetic screen for mutants resistant to the ATP-competitive TOR inhibitor AZD-8055. The eukaryotic TOR (Target of Rapamycin) kinase is emerging as a major hub controlling growth responses in plants largely thanks to the use of ATP-competitive inhibitors. We identified a dominant mutation in the DFG motif of the Arabidopsis TOR kinase domain that leads to very strong resistance to AZD-8055. This resistance was characterized by measuring root growth, photosystem II (PSII) activity in leaves and phosphorylation of YAK1 (Yet Another Kinase 1) and RPS6 (Ribosomal protein S6), a direct and an indirect target of TOR respectively. Using other ATP-competitive TOR inhibitors, we also show that the dominant mutation is particularly efficient for resistance to drugs structurally related to AZD-8055. Altogether, this proof-of-concept study demonstrates that a pharmacogenetic screen in Arabidopsis can be used to successfully identify the target of a kinase inhibitor *in vivo* and therefore to demonstrate inhibitor specificity. Thanks to the conservation of kinase families in eukaryotes, and the possibility of creating amino acid substitutions by genome editing, this work has great potential for extending studies on the evolution of signaling pathways in eukaryotes.

Keywords: TOR, signaling, ATP-competitive kinase inhibitor, AZD-8055, screen, resistant mutant, YAK1, RPS6, plant growth, photosynthesis.

INTRODUCTION

Kinases are major components of signaling pathways that control through phosphorylation essential aspects of cellular activities such as cell growth, division, and differentiation in all organisms. In recent years, studies of mammalian kinases have taken advantage of the development of new kinase inhibitors. Inhibitors are tools that are complementary to genetic approaches in functional studies, and they also come with unique advantages such as their ability to rapidly, robustly, and reversibly inhibit a kinase in tissues or cell types to reveal spatiotemporal features of target inhibition (Arrowsmith et al., 2015). However, in order to be used to study the actors of signaling pathways, these inhibitors must be both potent and selective. Selectivity, the capacity of a drug to inhibit a single target or a family of targets without inhibiting other kinases, is essential to perform accurate functional studies while avoiding misleading results and is generally evaluated *via* large-scale *in vitro* inhibition assays or *in vitro* interaction maps (Arrowsmith et al., 2015; Bain et al., 2007; Chresta et al., 2010; Fabian et al., 2005). However, such information cannot fully rule out putative off-target effects of drugs *in vivo*. The obtention of a mutant of a kinase resistant to drug concentrations that inhibit the wild-type kinase has therefore been proposed as the "gold standard" or the "ultimate confirmation" to identify the on-target effects of a kinase inhibitor *in vivo* (Kung & Shokat, 2005; Persky et al., 2020). An excellent example of the importance of drug resistance mutations in drug target identification is the yeast TARGET OF RAPAMYCIN (TOR) kinase identified by means of mutations conferring resistance to rapamycin (Heitman et al., 1991). One such

mutation affected the FKBP12-Rapamycin Binding (FRB) domain of TOR, and when introduced into the mammalian TOR coding sequence demonstrated that the effects of rapamycin were due to TOR inhibition in mammalian cells (Brunn et al., 1997). This work paved the way for a plethora of studies deciphering the essential role of the mammalian TOR pathway in the control of cell growth, proliferation, and metabolism (Sabatini, 2017). More recently, mutants resistant to ATP-competitive inhibitors have been developed for characterizing the *in vivo* targets of mammalian kinases such as Aurora A, ULK1, CDK2, and CDK4/6 (Echalier et al., 2012; Persky et al., 2020; Petherick et al., 2015; Sloane et al., 2010).

Although chemical biology is less developed in plants compared to animal studies, the use of small molecules to study biological processes is increasing in plants, with a particular interest in signaling pathways (De Rybel et al., 2009; Ercoli et al., 2022; Hicks & Raikhel, 2014; Liu et al., 2023; Malinovsky et al., 2017; Montané & Menand, 2019; Saito et al., 2022; Takáč et al., 2013; Wu et al., 2019). Most kinase inhibitors used in plants were first developed for animal cells and selectivity experiments were originally performed on animal kinases. Therefore, even if kinase domains are generally well conserved (Zulawski et al., 2014), the selectivity of these inhibitors towards plant kinases could be questionable, reinforcing the need for drug-resistant mutants in plants. In this study, we addressed this issue with a pharmacogenetic screen for identification of the kinase direct target of a drug in the model plant *Arabidopsis thaliana* (Arabidopsis). We performed this work on the TOR kinase because several ATP-competitive TOR inhibitors have been proven to be potent in plants (Montané & Menand, 2013), and because the TOR pathway is central to the regulation of plant growth (McCready et al., 2020). Together with the checkpoint kinases Ataxia-Telangiectasia Mutated (ATM) and Ataxia- and Rad3-related (ATR), TOR belongs to the small Phosphatidylinositol-3-Kinase-Related-Kinase (PIKK) family. Highly selective inhibitors have been obtained for each PIKK, and pan-PIKK inhibitors have also been developed (Chresta et al., 2010; Hsieh et al., 2012; Liu et al., 2013; Mao et al., 2022; Stakyte et al., 2021; Yu et al., 2010). While rapamycin is not efficient in wild type (WT) plants, potent ATP-competitive TOR inhibitors have been used extensively in recent studies aiming to decipher the plant TOR signaling pathway but their selectivity were not yet fully adressed in plants (Henriques et al., 2022; Montané & Menand, 2019). We used the ATP-competitive inhibitor AZD-8055 for our pharmacogenetic screen because its selectivity to TOR (approx. 1000-fold) was demonstrated in an assay against all class I phosphatidylinositol 3-kinase (PI3K) isoforms and other members of the PIKK family (Chresta et al., 2010), and because its action is highly reproducible and robust in plants (Montané & Menand, 2019).

Here we demonstrate that a dominant mutation in the DFG motif of plant TOR kinase domain leads to strong resistance to the selective ATP-competitive TOR inhibitor AZD-8055. TOR inhibition was monitored by measuring root growth inhibition, the disappearance of phosphorylation from the direct TOR target YET ANOTHER KINASE 1 (YAK1) and the indirect TOR target RIBOSOMAL PROTEIN S6 (RPS6), and inhibition of photosystem II (PSII) activity. Using different inhibitors, we also show that this TOR mutation confers resistance to TOR inhibitors structurally related to AZD-8055. This proof-of-concept work shows that a pharmacogenetic screen can be used to identify the direct target of a drug in Arabidopsis.

RESULTS

A pharmacogenetic screen identifies *tor-15*, a dominant *TOR* mutant highly resistant to AZD-8055

In this study, we characterized a new mutant originally isolated in the same screen that allowed the identification of three *YAK1* mutants (Barrada et al., 2019). Arabidopsis Col^{er105} EMS (ethyl methanesulfonate) mutants were germinated on medium supplemented with 1 μM AZD-8055 a concentration that triggered a strong root growth inhibition (GI) of 75% (hereafter GI_{75}). Among the mutants growing at least twice as much as the parental line, one showed particularly strong resistance. Analysis of the F2 progeny obtained by a backcross of the resistant mutant with Col^{er105} revealed a segregation of 3 AZD-8055 resistant plants to 1 sensitive, indicating that the mutation responsible for the resistance to AZD-8055 is dominant (Figure S1). We used a Next-Generation-Mapping strategy to identify the causal mutation and found that a mutation in the *TOR* gene co-segregates with the drug resistance phenotype (Figure S2) (Austin et al., 2011). This mutant was named *tor-15*, following the 14 *TOR* T-DNA mutants already described (Menand et al., 2002; Ren et al., 2011). Further analyses showed that the *tor-15* mutation leads to the substitution of the glycine (G) of the DFG motif inside the ATP-binding clef of the TOR kinase domain by a glutamic acid (E) at position 2268 (Figure 1a; Figures S3 and S4). The aspartic acid (D) of the DFG motif is a negatively charged amino acid interacting with a magnesium ion (Mg^{2+}) that itself interacts with a phosphate of the ATP molecule (Baretić & Williams, 2014; Nagar, 2007; Van Der Wolk et al., 1995). We could therefore predict that the substitution of the G by an E in *tor-15* would increase the negative charge of the DFG motif. Indeed, comparative modeling indicates that the G2268E substitution is very close to the ATP binding site (Figure S4) and could thus have an impact on ATP and AZD-8055 binding, for instance by increasing the negative charge or the steric hindrance. After the first backcross to the parental Col^{er105} line, *tor-15* was further backcrossed 5 times to Col-0 WT in order to remove the *er105* mutation

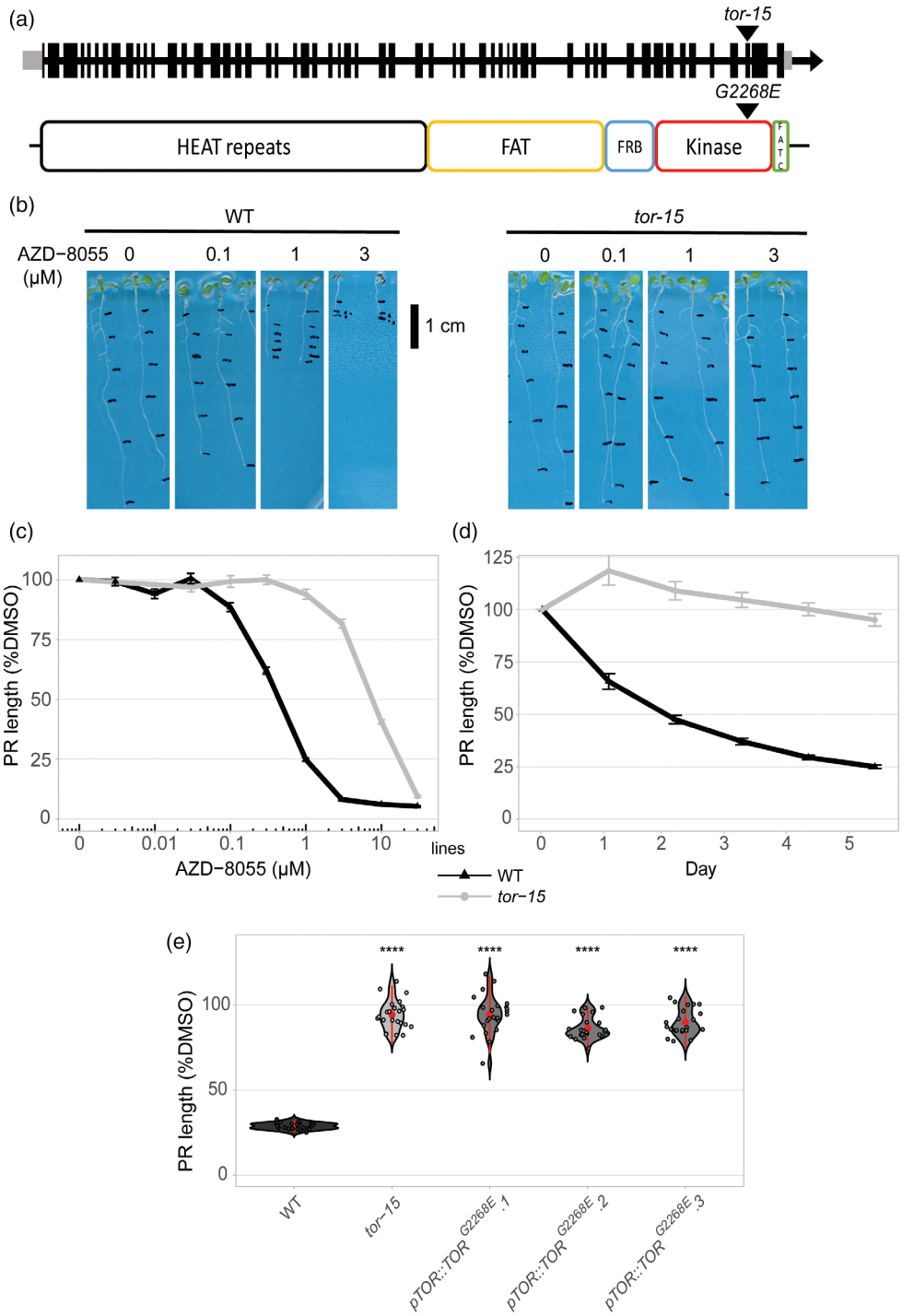

Figure 1. A mutation in the TOR kinase domain suppresses AZD-8055 mediated growth inhibition.
(a) Localization of the *tor-15* mutation in the *TOR* genomic sequence with exons represented by black boxes and position of the corresponding amino acid substitution (G2268E) in the TOR protein sequence.
(b) Pictures of WT and *tor-15* seedlings 5 days after transfer of 3-day-old plants onto media containing different AZD-8055 concentrations. Black marks were used to follow daily root growth. Scale bar, 1 cm.
(c) AZD-80555 dose–response curves of WT and *tor-15* seedlings 5 days after transfer onto drug-containing media. Primary root (PR) length is presented as a percentage of root length on DMSO (n = 21–24).
(d) Time course of PR growth after transfer to 1 μM AZD-8055 (n = 21–24). Full distribution of data from (c) and (d) are shown in Figure S5. (e) Root growth during 4 days after transfer of 4 days old plants onto 1 μM AZD-8055 for the WT, *tor-15*, and three independent transgenic lines transformed with a plasmid carrying the *pTOR::TOR*^{G2268E} genomic sequence (n = 23–24). Data are represented as violin plot showing the full distribution of the data. Red dot marks the mean, read lines the standard deviation, and gray dots all sample points.

The Plant Journal published by Society for Experimental Biology and John Wiley & Sons Ltd.,
The Plant Journal, (2023), doi: 10.1111/tpj.16564

and to reduce background EMS mutations. We confirmed by sequencing PCR products that the TOR^{G2268E} mutation was still present in backcrossed plants that were used for further experiments.

To further characterize the level of AZD-8055 resistance of *tor-15* (Figure 1b), we performed dose–response curves (Figure 1c) and time course of root growth (Figure 1d). The dose-response curve of *tor-15* was strongly shifted towards high AZD-8055 concentrations compared to WT (Figure 1c), showing a GI_{50} dose close to 7 μM, which was more than 17 times higher than the WT (0.4 μM). In addition, we observed that the growth of the aerial part of *tor-15* at 1 μM was also resistant to AZD-8055 as cotyledons and leaves grew like the WT without inhibitor, showing that this drug-resistance phenotype is not restricted to roots (Figure 1b). A time course experiment showed that the AZD-8055 resistance of *tor-15* is stable over time, highlighting the robustness of this AZD-8055 resistance phenotype (Figure 1d). In order to confirm that the G2268E mutation was responsible for the dominant AZD-8055 resistance phenotype of *tor-15*, we transferred the mutation into the WT. To do so, we amplified a 20 380 bp genomic *TOR* fragment ranging from the native promoter up to the 3′UTR from the genomic DNA of *tor-15*, cloned it into a binary vector, and used it to transform WT plants. Three independent transgenic lines were all strongly resistant to AZD-8055, in a similar manner to *tor*-15 (Figure 1e). This showed that the G2268E mutation is indeed the causal mutation responsible for AZD-8055 resistance in *tor-15*. We selected one of those lines (*pTOR::*TOR^{G2268E}*.1*) for further experiments and named it hereafter *pTOR::*TOR^{G2268E}.

These results demonstrate that our pharmacogenetic screen allowed the isolation of a dominant mutation in Arabidopsis *TOR* that confers a strong and robust resistance to the ATP-competitive TOR inhibitor AZD-8055. These findings are in line with the fact that the mutation is located within the TOR kinase domain that is indeed directly targeted by AZD-8055. This validates the selectivity of AZD-8055 towards plant TOR *in vivo*.

Immunodetection of YAK1 and RPS6 phosphorylation demonstrates that *tor-15* retains TOR activity under AZD-8055 treatment

One way to ascertain the *in vivo* efficiency of a kinase inhibitor is through analysis of targets that are known to be regulated by the catalytic activity of the kinase of interest. The YAK1 protein is directly phosphorylated by TOR at Ser847 and is as a repressor of growth that is itself repressed through phosphorylation by active TOR (Barrada et al., 2019; Forzani et al., 2019; Van Leene et al., 2019). To analyze changes in YAK1 phosphorylation in *tor-15*, we produced (*i*) an antibody against AtTOR in order to check any change of TOR amount in the mutant, (*ii*) an antibody against YAK1 (anti-YAK1) according to Huang et al., (40), and (*iii*) a novel antibody against the peptide carrying the phosphorylated Ser847 of YAK1 (anti-YAK1 pSer847). We showed that the anti-YAK1 (Figure S6a,b) and the anti-YAK1 pSer847 (Figure S6c) antibodies were able to detect their respective targets in seedlings of the *pYAK1::YAK1-GUS* transgenic line in which YAK1-GUS is expressed under the control of the *YAK1* promoter (Barrada et al., 2019). Time course analysis of the YAK1 pSer847 signal in response to 1 μM AZD-8055 showed a clear and progressive reduction of YAK1-GUS phosphorylation which reached a minimum after 24 h of treatment (Figure 2a; Figure S7) whereas the amount of YAK1-GUS hardly changed. This shows that our antibodies can clearly detect TOR-dependent YAK1-GUS phosphorylation. To study the phosphorylation of YAK1 in *tor-15*, the mutant was crossed with the *pYAK1::YAK1-GUS* line. Western blots showed that the *pYAK1::YAK1-GUS* and the *pYAK1::YAK1-GUS tor-15* lines had similar constitutive levels of TOR, YAK1-GUS, and YAK1-GUS pSer847 (Time 0 h, Figure 2b; Figures S8 and S9). After 24 h of treatment with 1 μM AZD-8055, the YAK1 pSer847 signal was only maintained when YAK1-GUS was in the *tor-15* background (Figure 2b; Figures S8 and S9). This demonstrates that in control conditions TOR activity in *tor-15* is constitutively similar to the WT but is maintained at a concentration of AZD-8055 high enough to strongly decrease TOR activity in the WT. This conclusion was also supported by experiments with ribosomal protein S6, an indirect target of TOR that is used as a readout of TOR activity (Dobrenel et al., 2016; Ingargiola et al., 2023) and whose phosphorylation on Ser 240 was maintained at a high level only in the *tor-15* mutant under AZD-8055 treatment (Figures 2c; Figures S10 and S11a,b). We also looked for the effect of Carbon/Nitrogen balance on the phosphorylation of RPS6 according to Ingargiola et al. (2023). When sucrose was added to sucrose-starved seedlings, WT and *tor-15* experienced a similar activation of RPS6 phosphorylation which was reduced by the inhibitor of glutamine synthase, glufosinate (Figure 2c; Figure S11a,b). When seedlings were sucrose- and nitrogen-starved, the addition of both sucrose and nitrogen was required to activate RPS6 phosphorylation in both WT and *tor-15* (Figure S11c, d). These data argue in favor of *tor-15* kinase responding like a WT kinase in terms of reactivity to carbon and nitrogen nutrients.

Next, we tested the influence of the *tor-15* background on the activity of the *SIAMESE-RELATED4* (*SMR4)* promoter which is activated in a YAK1-dependent manner during TOR inhibition (Barrada et al., 2019). GUS staining of seedlings carrying the *pSMR4::GUS* transcriptional fusion showed that *SMR4* was not induced by 1 μM AZD-8055 in *tor-15* (Figure 3; Figure S12). This indicates that a high concentration of AZD-8055 does not activate the signaling

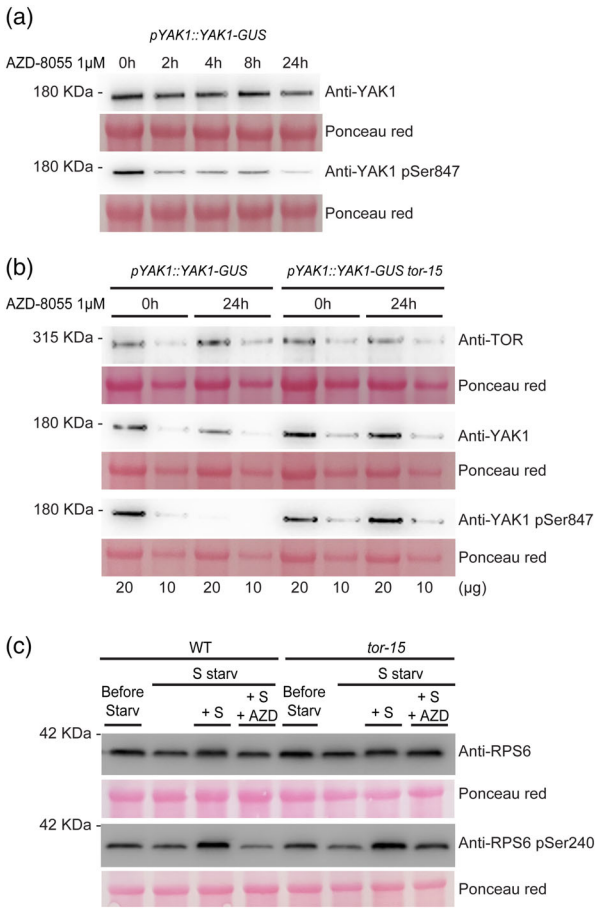

Figure 2. The *tor-15* mutant maintains YAK1 pSer847 and RPS6 phosphorylation under AZD-8055 treatment.
(a) Western blots showing the kinetics of AZD-8055-dependent YAK1 phosphorylation. *pYAK1::YAK1-GUS* plants were transferred at 7 days onto 1 μM AZD-8055 and sprinkled with 1 ml of 1 μM AZD-8055 in liquid growth medium. Seedlings were harvested at 2, 4, 8, and 24 h after treatment. Two antibodies were used: anti-YAK1 and anti-YAK1 pSer847. Complete blots are available in Figure S7. (b) Western blots against TOR, YAK1 and YAK1-pSer847 of YAK1-GUS and *tor-15* crossed with YAK1-GUS at 0 and 24 h of 1 μM AZD-8055 treatment. For each sample 20 and 10 μg of total proteins were loaded. Ponceau red staining is shown for each Western blot as an indicator of protein loading. Complete blots are available in Figure S8 and a replicate in Figure S9. (c) Western blots against RPS6 (maize) and RPS6-pSer240 of WT and *tor-15*. Proteins were loaded at 20 μg. Plants before Starvation (Before Starv) are shown next to plants sucrose-starved for 24 h (S Starv) and then treated for 5 h with sucrose-starvation media ±1% sucrose (Suc) and ±2 μM AZD-8055 (AZD). Complete blots are available in Figure S10.

pathway downstream of YAK1 in the *tor-15* background, which is in agreement with the maintenance of YAK1-GUS phosphorylation in this line (Figure 3).

Therefore, the *tor-15* mutation allows the TOR kinase to remain active and to phosphorylate the TOR direct target YAK1, and TOR indirect target RPS6, even in the presence of a high concentration of AZD-8055. This provides a molecular explanation for the observed resistance of root growth to AZD-8055 in *tor-15*.

The TOR^{G2268E} mutation confers selective plant resistance to different ATP-competitive TOR inhibitors

To test the extent of drug resistance of plants carrying the TOR^{G2268E} mutation, we followed the root growth of WT, *tor-15*, and the *pTOR::TOR^{G2268E}* line under treatment with different ATP-competitive TOR inhibitors. We chose TOR selective inhibitors whose structures are based on different skeletons (Mao et al., 2022) such as the morpholine-substituted heterocyclic-based inhibitors AZD-8055 and WYE-132, and the pyrazolo [3,4-d]pyrimidin-4-amine based inhibitor MLN0128 (hereafter INK128) (Hsieh et al., 2012; Yu et al., 2010). We also tested the quinolone-based inhibitor Torin2 which is a pan-PIKK selective inhibitor (Chopra et al., 2020; Liu et al., 2013). We tested these inhibitors at concentrations that caused a GI_{75} of the WT (Figure 4a–d) according to dose–response curves (Figure 1c; Figure S5) (Montané & Menand, 2013).

The root growth of the WT under 1 μM of AZD-8055 was severely impaired within the first 2 days leading to a plateau value of root growth inhibition of 75% 3–4 days later whereas both the *tor-15* and the *pTOR::TOR^{G2268E}* lines were unaffected during the first day and remained strongly resistant over time (Figure 4a). A response similar to AZD-8055 was observed with 0.6 μM WYE-132 indicating that the TOR^{G2268E} mutation confers strong and very similar resistance to different selective TOR inhibitors based on a morpholine-substituted heterocyclic skeleton (Figure 4b). *tor-15* and the *pTOR::TOR^{G2268E}* line were also resistant to INK128, although the level of resistance was lower than for AZD-8055 and WYE-132 (Figure 4c). In contrast, Torin2 was the sole drug that inhibited the growth of both the *tor-15* mutant and the *pTOR::TOR^{G2268E}* line during the first day of treatment and maintained this inhibition over time (Figure 4d). Hence, plants carrying the TOR^{G2268E} mutation were clearly less resistant to Torin2 than to AZD-8055 and WYE-132, and to a certain extent to INK128. In general, the *pTOR::TOR^{G2268E}* line was slightly but often significantly less resistant to TOR inhibitors than *tor-15* probably because it carries both WT and G2268E versions of *TOR* (Figure 4a–d; Table S2). Nevertheless, since all the drugs tested show a similar potency by inhibiting WT at a similar μM concentration range, these data reveal that the TOR^{G2268E} substitution is remarkably well adjusted to provide resistance to AZD-8055, the drug used for screening the mutant library, to the structurally-related WYE-132, and to a lesser extent, to INK128 which has a slightly different chemical-skeleton. The *tor-15* mutation appeared less effective in demonstrating that TOR is the target of the quinolone-based Torin2 *in vivo*. However, Torin2 is a pan-PIKK-selective inhibitor making it difficult to determine whether TOR inhibition alone or in combination with another PIKK was responsible for the phenotype observed (Chopra et al., 2020; Liu et al., 2013). Finally, both the

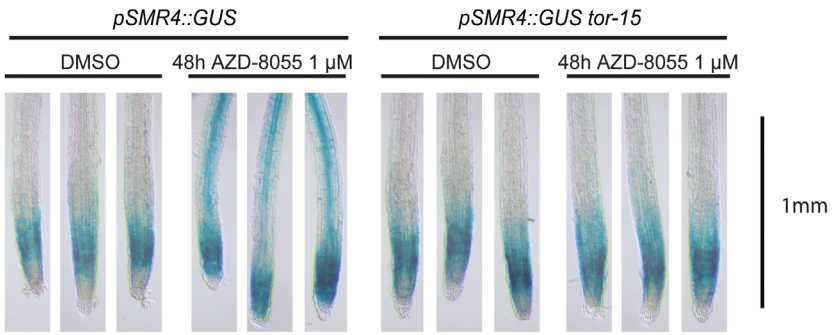

Figure 3. The *tor-15* mutant maintains low activity of the SMR4 promoter under AZD-8055 treatment. GUS staining of *pSMR4::GUS* and *pSMR4::GUS tor-15* for 4 h after 0 and 48 h of 1 µM AZD-8055 treatment. Scale bar, 1 mm. More pictures are available in Figure S12.

protein synthesis inhibitor cycloheximide and the CDK inhibitor roscovitin (Montané & Menand, 2013), similarly inhibited the growth of all three genotypes, indicating that the TOR^{G2268E} mutation does not confer resistance to growth inhibitors that are not TOR-selective (Figure 4e,f).

These data show that the TOR^{G2268E} mutation confers a particularly strong resistance to the morpholine-substituted heterocyclic skeleton inhibitors AZD-8055 and WYE-132. Thus, the combination of the mutant with its screening drug, AZD-8055 or the structurally related WYE-132, represents a perfect tool to study TOR-specific effects on plant.

The TOR^{G2268E} mutation prevents ATP-competitive TOR inhibitor-mediated inhibition of photosystem II

It was previously shown that TOR influences photosynthesis in plant and algae (D'Alessandro et al., 2023; Dong et al., 2015; Imamura et al., 2018; Sun et al., 2016; Upadhyaya & Rao, 2019). In order to test whether the TOR^{G2268E} mutation could confer resistance to TOR-inhibitor-induced changes in other processes than root growth, we investigated its effect on the maximal quantum efficiency of photosystem II (Fv/Fm), a parameter known to be inhibited in the presence of AZD-8055 (Sun et al., 2016; Upadhyaya & Rao, 2019). The Fv/Fm was measured in leaf discs cut from young, fully expanded rosette leaves. AZD-8055 dose dependence of Fv/Fm shows that WT PSII inhibition was triggered at similar doses to those that trigger root inhibition (Figure S14). These similar potencies suggest that this inhibitor similarly diffuse in both cut tissues and full seedlings. Indeed, similarly to 75% root growth inhibition of the WT, 1 µM AZD-8055 induced a maximal decrease of Fv/Fm (up to 50%) 3 days after treatment, indicating a highly depressed PSII activity. Meanwhile, *tor-15* and the *pTOR::TOR^{G2268E}* line maintained approximately 100% Fv/Fm with a strong and stable resistance to AZD-8055 (Figure 5a). Similar results were obtained with 0.6 µM of WYE-132 (Figure 5b), confirming an equivalent potency and TOR selectivity of AZD-8055 and WYE-132 in leaves as well as roots. In contrast, a higher concentration of INK-128 (40 µM) and Torin2 (10 µM) were required to affect Fv/Fm than root growth suggesting that both inhibitors have a greater tissue context dependence that may alter their efficacy towards TOR (Figure 5c,d; Figures S17–S19). Both *tor-15* and the *pTOR::TOR^{G2268E}* line behaved the same way showing the weakest resistance to Torin2 (Figure 5c,d; Figures S17–S19), similar to the results on roots. When we tested lincomycin, an inhibitor of chloroplast protein synthesis that does not act on TOR, the PSII QY of all lines was affected in the same way (Figure 5e). This result highlights the specificity of the TOR^{G2268E} mutation towards TOR inhibitors.

These data indicate that AZD-8055 and WYE-132, though not Torin2, repress the activity of PSII in leaf discs at similar doses to which they inhibit root growth. This demonstrates the consistently high potency of morpholine-substituted heterocyclic skeleton inhibitors in different tissues. The TOR^{G2268E} mutation confers strong resistance to PSII repression by AZD-8055 and WYE-132 demonstrating that it is a specific response to TOR inhibition. Only a slight resistance was observed for Torin2 highlighting again that the TOR^{G2268E} mutation appears less effective in conferring resistance to this quinolone-based inhibitor.

DISCUSSION

An ideal situation for functional studies of kinases *in vivo* is to have a potent and selective inhibitor and to confirm its primary target with inhibitor-resistant mutants (Echalier et al., 2012; Kung & Shokat, 2005; Persky et al., 2020; Sloane et al., 2010). The effect of an inhibitor observed on the WT can be interpreted as kinase-specific if it is not observed in the kinase-resistant mutant. Thanks to our pharmacogenetic screen in Arabidopsis, we obtained the ideal combination of an inhibitor and corresponding inhibitor-resistant mutant for the Arabidopsis TOR kinase. Using this combination, we could validate inhibitor specificity *in vivo* through growth experiments in roots, PSII activity assays in leaves, and detection of the phosphorylation of YAK1, a direct TOR target. The precision of the inhibitor/inhibitor-resistant mutant combination is highlighted by the fact the TOR^{G2268E} mutation confers a strong resistance to AZD-

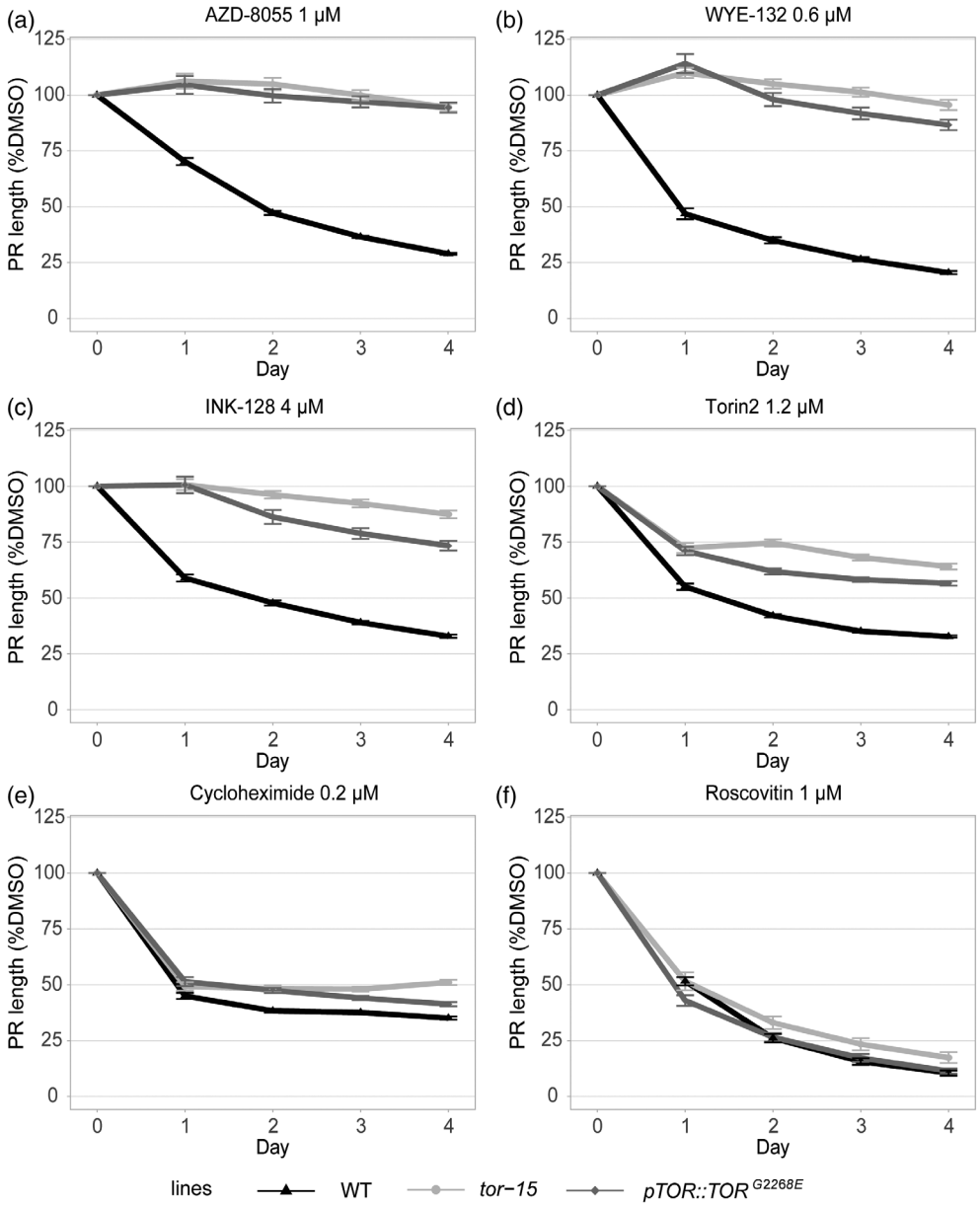

Figure 4. The TOR^{G2268E} mutation only confers resistance to ATP-competitive TOR inhibitors.
(a–e) Time course of PR growth of WT, *tor-15*, and the *pTOR::TOR*^{G2268E} line at the indicated concentrations of the TOR inhibitors AZD-8055 (a), WYE-132 (b), INK128 (c), and Torin2 (d), the protein synthesis inhibitor cycloheximide (e), and the pan-CDK inhibitor roscovitin (f). 4-day-old seedlings were transferred onto drug-containing media and their growth was monitored for 4 days. Data are expressed as a percentage of primary root length on DMSO (n = 21–24). Full distribution of data from (a–f) are shown in Figure S13.

8055 and WYE-132, two inhibitors based on the same structure, and weaker resistance to INK128 and especially Torin2 which have different backbone structures (Mao et al., 2022). The particularly weak resistance of *tor-15* to Torin2 could also be due to the inhibition of another PIKK in addition to TOR. However, we could also consider that TOR^{G2268E} does not efficiently exclude Torin2 due to its structure. In this case, other *TOR* mutations better adapted at preventing Torin2 binding could confer a stronger resistance to this inhibitor. Nevertheless, AZD-8055 and WYE-132 are both potent and selective ATP-competitive TOR inhibitors that can be used now in combination with the *tor-15*-resistant mutant to evaluate the specific TOR kinase-dependent effects observed *in vivo* in plants. This combination could also help re-evaluate the accuracy of some previously proposed plant TOR targets (Henriques et al., 2022). Knowing that the TOR sequence is well conserved in eukaryotes (Zhu et al., 2022) and that all TOR sequences analyzed have the DFG motif, this strategy can potentially be applied to other plants, or even to any other eukaryote by genome editing

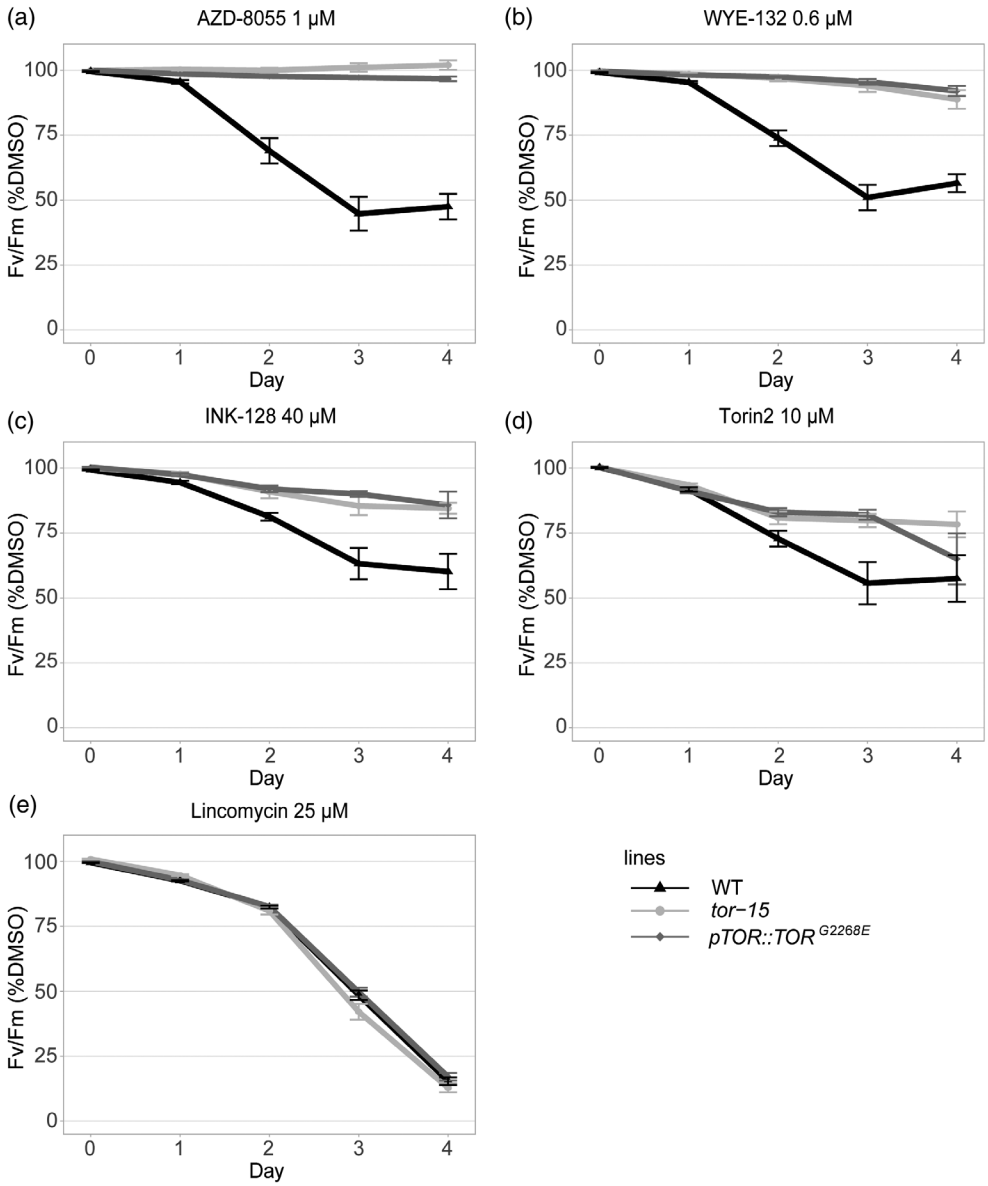

Figure 5. The TOR^{G2268E} mutation confers resistance to the TOR inhibitor-dependent decrease of photosystem II maximal efficiency.
(a–e) Time course of maximal efficiency of PSII (Fv/Fm) of WT, *tor-15*, and the *pTOR::TOR*^{G2268E} line after treatment of leaf discs with the indicated concentrations of the selective TOR inhibitors AZD-8055 (a), WYE-132 (b), INK-128 (c) and Torin2 (d), and the chloroplast translation inhibitor lincomycin (e). Leaf discs were harvested from 3-week-old plants and placed in 1.5 ml of drug-containing media for 4 days with daily measurements of Fv/Fm (n = 18). Data are presented as a percentage of Fv/Fm on DMSO. Full distribution of data from (a–e) are shown in Figure S16.

or by genetic transformation, as the resistance is conferred even in the presence of the WT alleles of TOR. Such approaches could therefore help understand the evolution of TOR functions among species. Taking a larger perspective, our pharmacogenetic screen which was based on resistance to drug-induced growth inhibition, could be easily adapted to any other kinase inhibitor affecting growth or indeed any other measurable parameter such as metabolite secretion, gene expression, or cell elongation (Malinovsky et al., 2017; Takáč et al., 2013; Wu et al., 2019) and therefore identify unambiguously its plant target *in vivo*. This approach can greatly increase elucidating the true actors of signaling pathways in general and is particularly important with the increased use of kinase inhibitors in plants (De Rybel et al., 2009; Echalier et al., 2012; Liu et al., 2023; Montané & Menand, 2013; Saito et al., 2022; Wu et al., 2019).

Although the phosphorylation of S6 kinases (S6K1 and S6K2) and their target the ribosomal protein S6 have been previously used to assess TOR activity, the plant community recently highlighted the need to develop alternative read-outs of TOR activity (Henriques et al., 2022). During this study, we developed novel antibodies enabling the

detection of the TOR-dependent phosphorylation of YAK1, a direct TOR target (Forzani et al., 2019; Van Leene et al., 2019). We think that YAK1 is a good candidate because it is one of the few direct TOR targets identified by both phosphoproteomics (Van Leene et al., 2019) and genetics, and because it plays an important role in regulating TOR-dependent growth at the whole plant level (Henriques et al., 2022; Van Der Wolk et al., 1995). We were only able to detect a tagged YAK1 protein. Detection of the endogenous YAK1 protein could be solved by identifying better polyclonal antibodies or selecting monoclonal antibodies. Nevertheless, immunodetection of YAK1 phosphorylation in *pYAK1::YAK1-GUS* is a new useful system for assessing TOR activity in plants that can be transferred in different mutant background by transformation or crossing.

A human *TOR* mutation leading to the same amino-acid substitution as *tor-15* was identified in a melanoma tumor and was shown to have increased TOR activity *in vitro* (Murugan et al., 2019). This mutation also induced TOR hyperactivation when transformed in NIH3T3 cells, and xenograft tumor formation in transformed nude mice. Although we did not see constitutive hyperphosphorylation of YAK1-GUS in *tor-15* under standard growth conditions or constitutive phosphorylation of RPS6 with the carbon and nitrogen nutrients conditions tested here, there is still a possibility that more TOR activity could be detectable in Arabidopsis *tor-15* mutant under other conditions or time course. In line with this hypothesis, a screen of mutations that confer resistance of CDK4 and CDK6 to the ATP-competitive inhibitor palbociclib in a human melanoma cell line identified a mutation in a hydrophobic pocket of the kinase domain that was further characterized as an activating mutation (Persky et al., 2020). Therefore, in addition to allowing the identification of drug targets, resistant mutants *per se* may help dissect the biological functions of kinases.

In conclusion, our pharmacogenetic screen allowed us to identify a novel *TOR* mutation that is a powerful tool for addressing the selectivity of ATP-competitive TOR inhibitors *in vivo*. Our work provides proof-of-concept for a strategy that could be applied to other kinases inhibitors and transferred to different organisms to study the evolution of eukaryotic signaling pathways.

EXPERIMENTAL PROCEDURES

Plant material

The *Arabidopsis thaliana* plants used for all the experiments except the mapping are in the Col-0 ecotype. The *tor-15* mutant was isolated from Col^{er105} EMS mutagenized seeds (Yi et al., 2014) screened on 1 μM AZD-8055 (Barrada et al., 2019) and was crossed once to Col^{er105} for mapping. However, the *erecta105* mutation was lost during further backcrosses with Col-0 WT done to clean the mutant from mutations not linked to the AZD-8055 resistance phenotype. We used the *tor-15* mutant backcrossed five times for Figure 1 and six times for other figures. The *pTOR::TOR*^{G2283E} lines were obtained from the transformation of WT Col-0 and are homozygous for the construction. The YAK1-GUS and pSMR4::GUS lines were described previously (Barrada et al., 2019; Yi et al., 2014). The *pYAK1::YAK1-GUS* and *pSMR4::GUS* constructs were introduced into the *tor-15* background by crossing with a *tor-15* mutant previously backcrossed five times.

Mutant screening and mapping by next-generation sequencing

The screening of mutants resistant to 1 μM AZD-8055 was described in Barrada et al. (2019). Next-generation sequencing (NGS) and analysis was also done according to Barrada et al. (2019), except that we sequenced a pool of 40 F2 plants for mapping (Figure S2) and used an Illumina Hiseq 4000 for NGS.

In vitro growth conditions and drug treatments

Seedlings were grown on solid medium prepared as described previously (Montané & Menand, 2013) with the addition of 2.5 mM of 2-(N-morpholino) ethanesulfonic acid (MES) to buffer the pH (5.5). Drugs were dissolved in pure DMSO (Euromedex, Souffelweyersheim, France) and sterilized with a 0.2 μM filter. The final DMSO concentration was 0.1% in control and drug-containing Petri dishes (Montané & Menand, 2013). Petri dishes containing 25 ml of medium were used and placed vertically to allow the roots to grow on the surface of the medium. Seeds were surface sterilized and placed at 4°C for 48 h. For Figure 1a–d, seeds were germinated for 3 days on media without DMSO before the transfer of seedlings to a drug-containing medium. For other experiments following root growth (Figure 1e and 4), seeds were germinated for 4 days before transfer. For TOR and YAK1 Western blots, we used 7 days-old untreated seedlings (t0), or seedlings transferred on AZD-8055 containing solid media for the time indicated.

For RPS6 phosphorylation experiments, the culture medium was from Barrada et al. (2019) modified according to Ingargiola et al. (2023), in which calcium nitrate was replaced by 2 mM $CaCl_2$ and glucose replaced by sucrose. KNO3, KCl (used to provide K when KNO3 was reduced), and sucrose concentrations were 1 mM KNO3, 4 mM KCl, 0.3% Sucrose in germination medium (Before Starv), 5 mM KNO3, 0 mM KCl and 0% sucrose in Sucrose-starvation medium (S Starv), and 0 mM KNO3, 5 mM KCl and 0% sucrose in Sucrose and Nitrogen-starvation medium (N and S Starv). AZD-8055 dissolved in DMSO was used at the final concentration of 2 μM in 0.1% DMSO. Glufosinate (GFA, Sigma-Aldrich, Saint Louis, MO, USA) dissolved in water was used at the final concentration of 27 μM. After 48 h in the dark at 4°C, seeds were grown vertically on a 5 g/L phytagel-solidified germination medium. 5-day-old seedlings were transferred with tweezers in wells of six-well plates (60 seedlings /well) containing 5 ml of appropriate liquid starvation medium for 24 h, then quickly rinsed in 4 ml and incubated for 5 h in 5 ml of the appropriate liquid media.

For all *in vitro* experiments, a photoperiod of 16 h at 23°C (90 μmol photons $m^{-2}.sec^{-1}$) was followed by 8 h of dark at 18°C. We purchased AZD-8055 and WYE-132 from Chemdea, Ridgewood, NJ, USA (CD0348 and CD0325), INK128 from Selleckchem (S2811), Torin2 from Tocris Biosciences, Bristol, UK (1223001-51-1) and cycloheximide and roscovitin from Sigma-Aldrich (66-81-9 and 186692-46-6).

Root growth measurements

The position of the tip of each primary root was marked every day on the back of the Petri dish. Five days after transfer to the new medium containing drug(s) or DMSO, Petri dishes were scanned

(Epson Perfection 1250, EPSON TWAIN5 software, Epson, Suwa, Japan) and primary root growth was measured using ImageJ software.

Plant growth on soil and Fv/Fm measurements

Plants were placed in a culture chamber with a photoperiod of 16 h at 22–23°C (130 μmol photons m^{-2}.sec^{-1}) followed by 8 h of dark at 18°C. After 3 weeks, leaf discs were cut from leaves of rank 4–6 with a 7 mm hole punch. Discs were disposed in 24 wells plate containing 1.5 ml of deionized water containing 0.1% DMSO and 0.01% Tween 20 (Sigma-Aldrich), with or without drug at different concentrations, except for the 40 μM INK-128 treatment which was at 0.2% of DMSO. Fv/Fm measurements were performed at the same time every day over 4 days. Prior to measurement, plates containing leaf discs were placed in the dark for 30 min, and measurements were performed with a Fluorcam FC 800-O imaging fluorometer (Photon System Instruments).

Cloning and plant transformation

The *pTOR::TOR*^{G2283E} construct was made by amplifying a 20 380 bp genomic fragment ranging from 2652 bp before the *TOR* START codon to 734 bp after the *TOR* STOP codon using *tor-15* genomic DNA as a matrix and primers AtTORg Forward (5′-GCCTTAATTAACGACGATGATGCGTACGAAAGAG-3′) and AtTORg Reverse (5′-ATAGGCGCGCCCGCATTTGAGAGAGTGGTAACGTA-3′). The amplification was performed with PrimeSTAR GXL DNA polymerase (#R050A, Takara Bio, Kusatsu, Japan) and then purified using the NucleoTraP CR kit (Macherey-Nagel, Duren, Germany, #740587). The purified PCR product was introduced into plasmid PMDC99 using *Asc*I/*Pac*I restriction sites and the DNA ligation kit LONG (Takara Bio #6024). *pTOR::TOR*^{G2283E} was transformed into Arabidopsis by floral dip and transgenic plants were selected on 50 μM hygromycin. Among five independent T2 lines homozygous for the transgene, three lines resistant to AZD-8055 were used in Figure 1e.

Antibody production and Western blotting

The anti-TOR antibody was produced according to Shin et al. (2019) by the manufacturer CliniSciences SAS (Nanterre, France). The anti-YAK1 antibody was produced according to Huang et al. (2017) by Proteogenix (Schiltigheim, France). The anti YAK1pSer847 was produced from the peptide Cys-QVETG(Sp) PPSNDPH by Proteogenix. For TOR and YAK1 Western blots, seedlings were ground in liquid nitrogen and then transferred into an extraction buffer adapted from Shin et al. (2019) (100 mM Tris–HCl pH 6.8, 1 mM EDTA pH 8, 5% SDS, 8 M Urea) by adding 0.5% phosphatase inhibitor cocktail 3 (Sigma-Aldrich, P0044), Protease inhibitor Cocktail (Roche Diagnostics, Mannheim, Germany, ref. 05892791001), 20 μM NaF and 50 μM MG132. The mixture was heated for 10 min at 50°C and centrifuged at 21300 ***g*** for 10 min in order to retain the supernatant. Protein concentration was measured with the Pierce™ 660 nm Protein Assay Reagent (ThermoFisher, Waltham, MA, USA ref. 22 660) supplemented with the Ionic Detergent Compatibility Reagent (IDCR) (ThermoFisher, #22663). Normalized protein extracts were supplemented with 2% beta-mercaptoethanol and 0.00125% bromophenol blue and then heated at 50°C for 2 min. Protein extracts were loaded onto a NuPAGE 4–12% Bis Tris gel (Invitrogen, Carlsbad, CA, USA, #NP0321BOX) and run at 90 V for 135 min in a running buffer consisting of 50 mM MES, 50 mM Tris base, 0.1% SDS, and 1 mM EDTA, pH 7.3. Protein gels were transferred onto Amersham™ Protran™ 0.45 μM nitrocellulose membranes (#10600002) using a Bio-Rad (Hercules, CA, USA) Trans-Blot Turbo Transfer System (#1704150). After staining with Ponceau red, membranes were blocked with a milk solution (TBS 1X, 50 g/L milk powder and 0.2% Tween 20) and then probed with either anti-TOR rabbit polyclonal anti-serum (dilution 1/1000), anti-YAK1 rabbit polyclonal anti-serum (dilution 1/1000) or anti-YAK1-pSer847 rabbit polyclonal anti-serum (dilution 1/1000). The anti-rabbit IGG-HRP (dilution 1/2000) was used as secondary antibody (Cell Signalling, Danvers, MA, USA, #7074S). All antibodies were diluted in the milk solution. The signal was revealed with a Chemiluminescent HRP Substrate (Millipore, Burlington, MA, USA, #WBKLS0500).

For RPS6 Western blots, 60 seedlings were quickly wrung out on a filter paper, put in an Eppendorf tube, and frozen in liquid nitrogen. Extraction was done by crushing frozen seedlings quickly transferred in a Duall®, Kimble® 1 ml grinder (Dutscher, Bernolsheim, France) and immediately covered with 0.25 ml of 1x Laemmli buffer with 100 mM DTT, 0.5% phosphatase inhibitor cocktail 3 (Sigma-Aldrich, P0044), Protease inhibitor Cocktail (Roche, ref. 05892791001), and 50 μM MG132. After incubation at 100°C for 10 min, extracts were centrifuged for 10 min (23 100 ***g***) and the supernatant was stored at −80°C. Protein dosage was done as described above and 20 μg of total proteins were separated on a 12% SDS-PAGE and immunoblotted and revealed as described above. Anti-maize RPS6 antibody (Williams et al., 2003) (Figures 3c; Figure S10) or Anti-human RPS6 antibody (Cell Signaling REF 2317S) (Figure S11) and anti-S6P (Ser240) antibody (Dobrenel et al., 2016) were used at the 1/1000 dilutions.

Graphs preparation and statistical analysis

Statistical analysis was conducted in R (R Core Team, 2023) and custom R scripts are provided at github (https://github.com/cecile-lecampion/Perdoux-et-al). Statistical analyses were performed according to normality status. On normally distributed data we performed analysis of variance with post hoc Tukey test and on nonparametric data we performed the Kruskal–Wallis test with post hoc Dunn test from the rstatix package (Kassambara, 2023). Graphs were produced using the package ggplot2 (Wickham, 2016). Error bars represent standard errors in graphs and histograms.

TOR kinase domain structure modeling

I-TASSER was employed to predict the kinase domain structures of WT and *tor-15* TOR (Yang & Zhang, 2015) using the crystal structure of mTORΔN-mLST8-ADP-MgF_3-Mg_2 (Yang et al., 2013) as template (PDB reference: 4JSV). The MgF_3-binding (Graham et al., 2002) was determined with I-TASSER from the 4JSV template by global and local structure comparisons (Yang & Zhang, 2015).

ACKNOWLEDGMENTS

This work was supported by a CEA DRF doctoral fellowship for R.P. and funding from the Agence Nationale de la Recherche funding (ANR-14-CE19-0007 and ANR-20-CE20-0027). We thank T. Desnos for EMS mutagenized seeds, Fabienne Granier and Raphaël Mercier for help with NGS data analysis, Julia Bailey-Serres and Alan Williams for the anti-RPS6 antibody, Christian Meyer for the anti-RPS6 pSer240 antibody, Ben Field for help with Fv/Fm measurements and for critical reading of the manuscript, Muriel Reissolet and Patrice Crété for managing the plant growth chambers, and Lieven De Veylder for *pSMR4::GUS* seeds.

CONFLICT OF INTEREST

The co-authors declare no conflict of interest.

AUTHOR CONTRIBUTIONS

RP, M-HM, and BM designed research; RP, AB, MB, CG, CB, MHM, and BM performed research; RP, CL, AB, M-HM, and BM analyzed data; RP, M-HM, and BM wrote the paper.

SUPPORTING INFORMATION

Additional Supporting Information may be found in the online version of this article.

Figure S1. Resistance to AZD-8055 segregates like a dominant trait in the *tor-15* mutant.

Figure S2. Mapping of the mutation responsible for AZD-8055 resistance in the *tor-15* mutant.

Figure S3. The DFG motif of the activation loop is highly conserved in TOR proteins.

Figure S4. The *tor-15* mutation is located inside the ATP-binding cleft.

Figure S5. Related to Figure 1c,d. Violin plot representation of the data from Figure 1c,d.

Figure S6. Development of antibodies to follow TOR-dependent YAK1 phosphorylation.

Figure S7. Related to Figure 2a. Full Western blots of AZD-8055 kinetic.

Figure S8. Related to Figure 2b. Full Western blot for TOR amount and YAK1 phosphorylation.

Figure S9. Related to Figure 2b. Repetition of Western blots for TOR amount and YAK1 phosphorylation.

Figure S10. Related to Figure 2c. Full Western blots for RPS6 protein phosphorylation.

Figure S11. Additional Western blots for RPS phosphorylation confirming the responses of *tor-15* to AZD and testing additional growth conditions.

Figure S12. Related to Figure 3. Additional set of Images of GUS staining of *pSMR4::GUS* in the WT or tor-15 background after treatment with AZD-8055.

Figure S13. Related to Figure 4. Violin plot representation of the data from Figure 4.

Figure S14. AZD-8055 dose-dependent effect on the maximum quantum yield (Fv/Fm) of WT and *tor-15* leaf discs.

Figure S15. INK128 dose-dependent effect on primary root growth.

Figure S16. Related to Figure 4. Violin plot representation of curves from Figure 5.

Figure S17. Effect of different doses of INK-128 on Fv/Fm.

Figure S18. Violin plot representation of the curves from Figure S17.

Figure S19. Effect of different doses of Torin2 on Fv/Fm.

Figure S20. Violin plot representation of the curves from Figure S19.

Table S1. Raw data for Figures 1c–e, 4, 5, S14, S15, S17, and S19.

Table S2. Statistical analysis for Figures 1c–e, 4, 5, S14, S15, S17, and S19.

REFERENCES

Arrowsmith, C.H., **Audia, J.E.**, **Austin, C.**, **Baell, J.**, **Bennett, J.**, **Blagg, J. *et al.*** (2015) The promise and peril of chemical probes. *Nature Chemical Biology*, **11**, 536–541.

Austin, R.S., **Vidaurre, D.**, **Stamatiou, G.**, **Breit, R.**, **Provart, N.J.**, **Bonetta, D. *et al.*** (2011) Next-generation mapping of Arabidopsis genes. *Plant Journal*, **67**, 715–725.

Bain, J., **Plater, L.**, **Elliott, M.**, **Shpiro, N.**, **Hastie, C.J.**, **Mclauchlan, H. *et al.*** (2007) The selectivity of protein kinase inhibitors: a further update. *Biochemical Journal*, **408**, 297–315.

Baretić, D. & **Williams, R.L.** (2014) The structural basis for mTOR function. *Seminars in Cell & Developmental Biology*, **36**, 91–101.

Barrada, A., **Djendli, M.**, **Desnos, T.**, **Mercier, R.**, **Robaglia, C.**, **Montané, M.-H. *et al.*** (2019) A TOR-YAK1 signaling axis controls cell cycle, meristem activity and plant growth in *Arabidopsis*. *Development*, **146**, dev171298.

Brunn, G.J., **Hudson, C.C.**, **Sekulic, A.**, **Williams, J.M.**, **Hosoi, H.**, **Houghton, P.J. *et al.*** (1997) Phosphorylation of the translational repressor PHAS-I by the mammalian target of rapamycin. *Science*, **277**, 99–101.

Chopra, S.S., **Jenney, A.**, **Palmer, A.**, **Niepel, M.**, **Chung, M.**, **Mills, C. *et al.*** (2020) Torin2 exploits replication and checkpoint vulnerabilities to cause death of PI3K-activated triple-negative breast cancer cells. *Cell Systems*, **10**, 66–81.e11.

Chresta, C.M., **Davies, B.R.**, **Hickson, I.**, **Harding, T.**, **Cosulich, S.**, **Critchlow, S.E. *et al.*** (2010) AZD8055 is a potent, selective, and orally bioavailable ATP-competitive mammalian target of rapamycin kinase inhibitor with in vitro and in vivo antitumor activity. *Cancer Research*, **70**, 288–298.

D'Alessandro, S., **Velay, F.**, **Lebrun, R.**, **Mehrez, M.**, **Romand, S.**, **Saadouni, R. *et al.*** (2023) Post-translational regulation of photosynthetic activity via the TOR kinase in plants. 2023.BioRxiv 05.05.539554.

De Rybel, B., **Audenaert, D.**, **Vert, G.**, **Rozhon, W.**, **Mayerhofer, J.**, **Peelman, F. *et al.*** (2009) Chemical inhibition of a subset of Arabidopsis thaliana GSK3-like kinases activates Brassinosteroid signaling. *Chemistry & Biology*, **16**, 594–604.

Dobrenel, T., **Mancera-Martinez, E.**, **Forzani, C.**, **Azzopardi, M.**, **Davanture, M.**, **Moreau, M. *et al.*** (2016) The Arabidopsis TOR kinase specifically regulates the expression of nuclear genes coding for Plastidic ribosomal proteins and the phosphorylation of the cytosolic ribosomal protein S6. *Frontiers in Plant Science*, **7**, 1611.

Dong, P., **Xiong, F.**, **Que, Y.**, **Wang, K.**, **Yu, L.**, **Li, Z. *et al.*** (2015) Expression profiling and functional analysis reveals that TOR is a key player in regulating photosynthesis and phytohormone signaling pathways in Arabidopsis. *Frontiers in Plant Science*, **6**, 677.

Echalier, A., **Cot, E.**, **Camasses, A.**, **Hodimont, E.**, **Hoh, F.**, **Jay, P. *et al.*** (2012) An integrated chemical biology approach provides insight into Cdk2 functional redundancy and inhibitor sensitivity. *Chemistry & Biology*, **19**, 1028–1040.

Ercoli, M.F., **Ramos, P.Z.**, **Jain, R.**, **Pilotte, J.**, **Dong, O.X.**, **Thompson, T. *et al.*** (2022) An open source plant kinase chemogenomics set. *Plant Direct*, **6**, e460.

Fabian, M.A., **Biggs, W.H.**, **Treiber, D.K. *et al.*** (2005) A small molecule–kinase interaction map for clinical kinase inhibitors. *Nature Biotechnology*, **23**, 329–336.

Forzani, C., **Duarte, G.T.**, **Van Leene, J.**, **Clément, G.**, **Huguet, S.**, **Paysant-Le-Roux, C. *et al.*** (2019) Mutations of the AtYAK1 kinase suppress TOR deficiency in Arabidopsis. *Cell Reports*, **27**, 3696–3708.e5.

Graham, D.L., **Lowe, P.N.**, **Grime, G.W.**, **Marsh, M.**, **Rittinger, K.**, **Smerdon, S.J. *et al.*** (2002) MgF3- as a transition state analog of phosphoryl transfer. *Chemistry & Biology*, **9**, 375–381.

Heitman, J., **Movva, N.R.** & **Hall, M.N.** (1991) Targets for cell cycle arrest by the immunosuppressant rapamycin in yeast. *Science*, **253**, 905–909.

Henriques, R., **Calderan-Rodrigues, M.J.**, **Luis Crespo, J.**, **Baena-González, E.** & **Caldana, C.** (2022) Growing of the TOR world. *Journal of Experimental Botany*, **73**, 6987–6992.

Hicks, G.R. & **Raikhel, N.V.** (2014) Plant chemical biology: are we meeting the promise? *Frontiers in Plant Science*, **5**, 455.

Hsieh, A.C., **Liu, Y.**, **Edlind, M.P.**, **Ingolia, N.T.**, **Janes, M.R.**, **Sher, A. *et al.*** (2012) The translational landscape of mTOR signalling steers cancer initiation and metastasis. *Nature*, **485**, 55–61.

Huang, W.-Y., **Wu, Y.-C.**, **Pu, H.-Y.**, **Wang, Y.**, **Jang, G.-J.** & **Wu, S.-H.** (2017) Plant dual-specificity tyrosine phosphorylation-regulated kinase optimizes light-regulated growth and development in Arabidopsis. *Plant, Cell and Environment*, **40**, 1735–1747.

Imamura, S., **Nomura, Y.**, **Takemura, T.**, **Pancha, I.**, **Taki, K.**, **Toguchi, K. *et al.*** (2018) The checkpoint kinase TOR (target of rapamycin) regulates expression of a nuclear-encoded chloroplast RelA-SpoT homolog (RSH)

and modulates chloroplast ribosomal RNA synthesis in a unicellular red alga. *Plant Journal*, **94**, 327–339.

Ingargiola, C., **Jéhanno, I.**, **Forzani, C.**, **Marmagne, A.**, **Broutin, J.**, **Clément, G. *et al.*** (2023) The Arabidopsis target of rapamycin kinase regulates ammonium assimilation and glutamine metabolism. *Plant Physiology*, **192**, 2943–2957.

Kassambara, A. (2023) rstatix: Pipe-Friendly Framework for Basic Statistical Tests. [Accessed June 27, 2023].

Kung, C. & **Shokat, K.M.** (2005) Small-molecule kinase-inhibitor target assessment. *Chembiochem*, **6**, 523–526.

Liu, H.-B., **Li, X.**, **Cai, J.**, **Jiang, L.L.**, **Zhang, X.**, **Wu, D. *et al.*** (2023) A screening of inhibitors targeting the receptor kinase FERONIA reveals small molecules that enhance plant root immunity. *Plant Biotechnology Journal*, **21**, 63–77.

Liu, Q., **Xu, C.**, **Kirubakaran, S.**, **Zhang, X.**, **Hur, W.**, **Liu, Y. *et al.*** (2013) Characterization of Torin2, an ATP-competitive inhibitor of mTOR, ATM, and ATR. *Cancer Research*, **73**, 2574–2586.

Malinovsky, F.G., **Thomsen, M.-L.F.**, **Nintemann, S.J.**, **Jagd, L.M.**, **Bourgine, B.**, **Burow, M. *et al.*** (2017) An evolutionarily young defense metabolite influences the root growth of plants via the ancient TOR signaling pathway. *eLife*, **6**, e29353.

Mao, B., **Zhang, Q.**, **Ma, L.**, **Zhao, D.-S.**, **Zhao, P.** & **Yan, P.** (2022) Overview of research into mTOR inhibitors. *Molecules*, **27**, 5295.

McCready, K., **Spencer, V.** & **Kim, M.** (2020) The importance of TOR kinase in plant development. *Frontiers in Plant Science*, **11**, 16.

Menand, B., **Desnos, T.**, **Nussaume, L.**, **Berger, F.**, **Bouchez, D.**, **Meyer, C. *et al.*** (2002) Expression and disruption of the Arabidopsis TOR (target of rapamycin) gene. *Proceedings of the National Academy of Sciences USA*, **99**, 6422–6427.

Montané, M.-H. & **Menand, B.** (2013) ATP-competitive mTOR kinase inhibitors delay plant growth by triggering early differentiation of meristematic cells but no developmental patterning change. *Journal of Experimental Botany*, **64**, 4361–4374.

Montané, M.-H. & **Menand, B.** (2019) TOR inhibitors: from mammalian outcomes to pharmacogenetics in plants and algae. *Journal of Experimental Botany*, **70**, 2297–2312.

Murugan, A.K., **Liu, R.** & **Xing, M.** (2019) Identification and characterization of two novel oncogenic mTOR mutations. *Oncogene*, **38**, 5211–5226.

Nagar, B. (2007) c-Abl tyrosine kinase and inhibition by the cancer drug imatinib (Gleevec/STI-571). *The Journal of Nutrition*, **137**, 1518S–1523S.

Persky, N.S., **Hernandez, D.**, **Do Carmo, M.**, **Brenan, L.**, **Cohen, O.**, **Kitajima, S. *et al.*** (2020) Defining the landscape of ATP-competitive inhibitor resistance residues in protein kinases. *Nature Structural and Molecular Biology*, **27**, 92–104.

Petherick, K.J., **Conway, O.J.**, **Mpamhanga, C.**, **Osborne, S.A.**, **Kamal, A.**, **Saxty, B. *et al.*** (2015) Pharmacological inhibition of ULK1 kinase blocks mammalian target of rapamycin (mTOR)-dependent autophagy. *Journal of Biological Chemistry*, **290**, 11376–11383.

R Core Team. (2023) *R: A language and environment for statistical computing*. Vienna, Austria: R Foundation for Statistical Computing. https://www.R-project.org/

Ren, M., **Qiu, S.**, **Venglat, P.**, **Xiang, D.**, **Feng, L.**, **Selvaraj, G. *et al.*** (2011) Target of rapamycin regulates development and ribosomal RNA expression through kinase domain in Arabidopsis. *Plant Physiology*, **155**, 1367–1382.

Sabatini, D.M. (2017) Twenty-five years of mTOR: uncovering the link from nutrients to growth. *Proceedings of the National Academy of Sciences USA*, **114**, 11818–11825.

Saito, A.N., **Maeda, A.E.**, **Takahara, T.T.**, **Matsuo, H.**, **Nishina, M.**, **Ono, A. *et al.*** (2022) Structure–function study of a novel inhibitor of cyclin-dependent kinase C in Arabidopsis. *Plant and Cell Physiology*, **63**, 1720–1728.

Shin, G.-I., **Moon, S.Y.**, **Jeong, S.Y.**, **Ji, M.G.**, **Cha, J.-Y.** & **Kim, W.-Y.** (2019) Production, characterization, and cross-reactivity of a polyclonal antibody against Arabidopsis TARGET OF RAPAMYCIN. *Applied Biological Chemistry*, **62**, 68.

Sloane, D.A., **Trikic, M.Z.**, **Chu, M.L.**, **Lamers, M.B.**, **Mason, C.S.**, **Mueller, I. *et al.*** (2010) Drug-resistant aurora A mutants for cellular target validation of the small molecule kinase inhibitors MLN8054 and MLN8237. *ACS Chemical Biology*, **5**, 563–576.

Stakyte, K., **Rotheneder, M.**, **Lammens, K.**, **Bartho, J.D.**, **Grädler, U.**, **Fuchß, T. *et al.*** (2021) Molecular basis of human ATM kinase inhibition. *Nature Structural and Molecular Biology*, **28**, 789–798.

Sun, L., **Yu, Y.**, **Hu, W.**, **Min, Q.**, **Kang, H.**, **Li, Y. *et al.*** (2016) Ribosomal protein S6 kinase1 coordinates with TOR-Raptor2 to regulate thylakoid membrane biosynthesis in rice. *Biochimica et Biophysica Acta (BBA) - Molecular and Cell Biology of Lipids*, **1861**, 639–649.

Takáč, T., **Pechan, T.**, **Šamajová, O.** & **Šamaj, J.** (2013) Vesicular trafficking and stress response coupled to PI3K inhibition by LY294002 as revealed by proteomic and cell biological analysis. *Journal of Proteome Research*, **12**, 4435–4448.

Upadhyaya, S. & **Rao, B.J.** (2019) Reciprocal regulation of photosynthesis and mitochondrial respiration by TOR kinase in Chlamydomonas reinhardtii. *Plant Direct*, **3**, e00184.

Van Der Wolk, J.P.W., **Klose, M.**, **De Wit, J.G.**, **Den Blaauwen, T.**, **Freudl, R.** & **Driessen, A.J.M.** (1995) Identification of the magnesium-binding domain of the high-affinity ATP-binding site of the Bacillus subtilis and Escherichia coli SecA protein. *Journal of Biological Chemistry*, **270**, 18975–18982.

Van Leene, J., **Han, C.**, **Gadeyne, A.**, **Eeckhout, D.**, **Matthijs, C.**, **Canoot, B. *et al.*** (2019) Capturing the phosphorylation and protein interaction landscape of the plant TOR kinase. *Nature Plants*, **5**, 316–327.

Wickham, H. (2016) Programming with ggplot2. In: *ggplot2*. Cham: Springer, pp. 241–253.

Williams, A.J., **Werner-Fraczek, J.**, **Chang, I.-F.** & **Bailey-Serres, J.** (2003) Regulated phosphorylation of 40S ribosomal protein S6 in root tips of maize. *Plant Physiology*, **132**, 2086–2097.

Wu, L., **Sadhukhan, A.**, **Kobayashi, Y.**, **Ogo, N.**, **Tokizawa, M.**, **Agrahari, R.K. *et al.*** (2019) Involvement of phosphatidylinositol metabolism in aluminum-induced malate secretion in Arabidopsis. *Journal of Experimental Botany*, **70**, 3329–3342.

Yang, H., **Rudge, D.G.**, **Koos, J.D.**, **Vaidialingam, B.**, **Yang, H.J.** & **Pavletich, N.P.** (2013) mTOR kinase structure, mechanism and regulation. *Nature*, **497**, 217–223.

Yang, J. & **Zhang, Y.** (2015) I-TASSER server: new development for protein structure and function predictions. *Nucleic Acids Research*, **43**, W174–W181.

Yi, D., **Alvim Kamei, C.L.**, **Cools, T.**, **Vanderauwera, S.**, **Takahashi, N.**, **Okushima, Y. *et al.*** (2014) The *Arabidopsis* SIAMESE-RELATED cyclin-dependent kinase inhibitors SMR5 and SMR7 regulate the DNA damage checkpoint in response to reactive oxygen species. *Plant Cell*, **26**, 296–309.

Yu, K., **Shi, C.**, **Toral-Barza, L.**, **Lucas, J.**, **Shor, B.**, **Kim, J.E. *et al.*** (2010) Beyond rapalog therapy: preclinical pharmacology and antitumor activity of WYE-125132, an ATP-competitive and specific inhibitor of mTORC1 and mTORC2. *Cancer Research*, **70**, 621–631.

Zhu, T., **Li, L.**, **Chang, H.**, **Zhan, J.** & **Ren, M.** (2022) Target of rapamycin regulates photosynthesis and cell growth in *Auxenochlorella pyrenoidosa*. *International Journal of Molecular Sciences*, **23**, 11309.

Zulawski, M., **Schulze, G.**, **Braginets, R.**, **Hartmann, S.** & **Schulze, W.X.** (2014) The Arabidopsis Kinome: phylogeny and evolutionary insights into functional diversification. *BMC Genomics*, **15**, 548.